Pol. J. Environ. Stud. Vol. XX, No. X (XXXX), 1-11
DOI: *10.15244/pjoes/207657* ONLINE PUBLICATION DATE: 2025-12-09

Original Research

Hydrochemical Characterization and Risk Implications of Sandstone Fissure Water in Qianyingzi Coal Mine, China: Insights for Sustainable Resource Management

Kai Yu[1], Jiying Xu[1]*, Hongbao Dai[2], Jie Ma[1], Hang Ma[1]

[1]School of Resources and Civil Engineering, Suzhou University, Suzhou, 234000Anhui, China
[2]School of Environment and Surveying and Mapping Engineering, Suzhou University, Suzhou, 234000, Anhui, China

Received: 30 April 2025
Accepted: 27 June 2025

Abstract

Hydrochemical analysis of groundwater reveals its composition and sources, providing a scientific basis for sustainable water resource utilization, ecological protection, and water-inrush disaster prevention. Moreover, water quality assessment not only determines groundwater suitability but also serves as a critical link connecting resource utilization, environmental conservation, and public health. To address these challenges, this study investigates 19 sandstone fissure water samples from the Qianyingzi Coal Mine. Hydrochemical characteristics were analyzed using ionic ratio analysis and statistical methods, whereas water quality assessment employed three distinct approaches: single-parameter assessment, F-value comprehensive evaluation, and fuzzy comprehensive evaluation. The resulting findings provide essential scientific support for strategies related to safe water usage, pollution control, and sustainable resource management in coal mining regions. The results indicate that anions in the fissure water are dominated by SO_4^{2-} and HCO_3^-, whereas cations primarily consist of Na^+ and K^+. The hydrochemical type is classified as $SO_4 \cdot HCO_3$-Na+K, reflecting the dominance of sulfate and bicarbonate anions combined with sodium and potassium cations. Furthermore, ionic ratio analysis revealed that the hydrochemical composition primarily stems from the dissolution and weathering of rock salt, as well as processes involving carbonate and sulfate minerals. Based on the F-value and fuzzy comprehensive evaluations, the fissure water was predominantly categorized as Class IV and V (according to national standards), signifying poor quality with potential environmental and health risks. These outcomes establish vital theoretical foundations and offer practical guidance for mitigating mine water hazards, optimizing groundwater exploitation, and enhancing ecological protection strategies in mining areas.

Keywords: sandstone fissure water, water chemistry characteristics, source analysis, Qianyingzi Coal Mine, water quality evaluation

*e-mail: jiyingxu1986@163.com
Tel.: +86-158-0557-4977

Introduction

Groundwater, a critical resource for maintaining ecosystem balance and supporting human societal development, requires an in-depth study of its chemical characteristics and evolution mechanisms. Such research can uncover material sources, transport pathways, and water-rock interactions, thereby forming the scientific foundation for assessing water resource availability and developing effective management strategies [1]. In coal mining areas, intensive anthropogenic activities drastically alter hydrogeological conditions. Specifically, chemical anomalies in fissure water in these regions are closely linked to water-inrush disasters and ecological degradation. Therefore, deciphering their genetic mechanisms is pivotal for ensuring mine safety and ecological restoration [2]. To address these challenges, water quality assessment has emerged as an extended approach. For example, fuzzy mathematical methods [3] dynamically integrate membership degrees and weights to quantify multi-factor synergistic effects, significantly enhancing the analytical capacity for complex water systems. Additionally, frameworks such as the World Health Organization (WHO) Water Quality Index (WQI) [4] and the European Union (EU) ecological risk assessment system provide critical references for managing high-salinity fissure water in mining areas.

Current research exhibits notable regional disparities. Domestically, studies primarily focus on high salinity and sulfate enrichment in coal mining areas. For instance, principal component analysis (PCA) [5] reveals that deep groundwater in Qianyingzi Coal Mine is influenced by rock salt dissolution and silicate weathering. However, quantitative assessments of mining impacts remain insufficient. Methodologically, clustering and correlation analyses [6] are widely applied to hydrochemical evolution studies, yet single-method approaches struggle to support systematic investigations of high-salinity fissure water. In contrast, international research emphasizes innovations in mineral dissolution kinetics and hydrogeochemical modeling. For example, multivariate statistical methods [7] analyze the synergistic effects of Himalayan glacial meltwater and rock weathering, while Gibbs diagrams [8] delineate evaporation-concentration dominance in the Dunhuang Basin. In the context of water quality assessment, fuzzy mathematics has gained traction for addressing nonlinear multi-indicator challenges, and clustering optimization models [9] are utilized for identifying mine water-inrush sources. Nevertheless, international studies predominantly focus on natural hydrological systems, with limited attention given to structurally complex coal mining areas. Moreover, existing models require enhanced adaptability to China's unique hydrogeological conditions, underscoring the need for deeper integration of regional research and global methodologies [10].

Located in the Xuzhou-Suzhou arcuate thrust tectonic belt of North China, Qianyingzi Coal Mine exhibits complex geological structures. Here, sandstone fissure water is characterized by high salinity and anomalous sulfate enrichment. As mining depth increases to 1,200 meters, roof and floor water inflow surges (peaking at 68.7 m^3/h), with dynamic hydrochemical variations posing severe challenges to roadway stability and water-inrush prevention. Although prior studies have preliminarily explored ion sources in deep groundwater, the quantitative contribution of ions remains inadequately resolved. Furthermore, current water quality assessments predominantly target shallow groundwater, with limited research on the deterioration processes of deep fissure water under mining disturbances.

To bridge these gaps, this study investigates sandstone fissure water from Qianyingzi Coal Mine using mathematical statistics, Piper trilinear diagrams, Gibbs diagrams, and ionic ratios. These methods aim to classify hydrochemical types and elucidate compositional characteristics and formation mechanisms. Additionally, single-parameter evaluation, the F-value method, and fuzzy comprehensive evaluation are employed to assess water quality grades and primary pollution factors. Ultimately, the research seeks to clarify the impact mechanisms of mining activities on the chemical evolution of fissure water, providing theoretical support for water hazard prevention, tiered water resource utilization, and ecological restoration in mining areas. This approach also offers a paradigm for hydrogeochemical studies in structurally complex coal mining regions.

Materials and Methods

Overview of the Study Area

Qianyingzi Coal Mine is located approximately 15 km southwest of Suzhou City's center, spanning the administrative regions of Suzhou City and Suixi County, Huaibei City. Geographically, it lies between longitudes 116°51′00″–117°00′00″ E and latitudes 33°27′00″–33°32′30″ N. The terrain is predominantly flat, with elevations ranging from +18.885 m to +24.720 m (averaging around +23 m), showing a gradual slope from higher elevations in the northwest to lower elevations in the southeast. Hydrologically, the Hui River – a tributary of the Huai River – traverses the central part of the mine. Specifically, the annual average water levels are +17.22 m upstream of Qixian Gate and +16.07 m downstream, with an average annual flow rate of 7.85 m^3/s at Linhuan upstream. Additionally, the area is intersected by an extensive network of artificial channels and dense agricultural irrigation systems.

Climatically, the region experiences a monsoon-influenced warm temperate semi-humid climate, characterized by distinct seasonal variations: mild temperatures with variable spring warmth, hot and rainy summers, crisp autumns, and cold, dry winters. Notably,

it benefits from abundant sunlight and a long frost-free period.

The groundwater within the study area is stratified into four distinct aquifers (groups) from the uppermost to the lowermost layers: the Cenozoic loose layer, the Permian main coal mining seam, the Taiyuan Formation limestone karstic fissured aquifer, and the Ordovician limestone karstic fissured aquifer. All samples were collected from the sandstone fractured aquifer associated with the top and bottom plates of the 32 coal seams. The burial depth of the floor varies between 187.95 and 1,206.83 meters, with an average of 592.09 meters. The thickness of the sandstone ranges from 0 to 130.60 meters, with a mean value of 21.08 meters. In this particular layer (section), the sandstone fractures are relatively well-developed yet exhibit a certain degree of heterogeneity. Specifically, the unified conversion values for q range from 0.0002 to 0.06445 L/(s•m), indicating weak water-bearing properties, and for k, they range from 0.00025 to 0.06157 m/d. Fig. 1 illustrates the geological relationship map of the study area along with the sample collection points.

Sample Collection and Processing

A total of 19 sandstone fissure water samples were collected from the study area. The 19 water samples were taken from various leak points at the mine face, with four collected from surface boreholes and seven and eight samples from rock workings on the east and west flanks, respectively.

During sampling, the following standardized procedures were implemented: Pre-rinsing: Sampling buckets were rinsed three times with deionized water. Field rinsing: Before collection, each bucket was rinsed three times with the sampled water to minimize contamination. Transport and storage: Samples were transported to the laboratory within 24 hours, filtered through 0.45 μm membranes, and stored at 4ºC for subsequent analysis.

Analytical methods included: pH and TDS: Measured using a portable OHAUS instrument. Cations (Na^+, K^+, Ca^{2+}, Mg^{2+}): Analyzed via an ISC-600

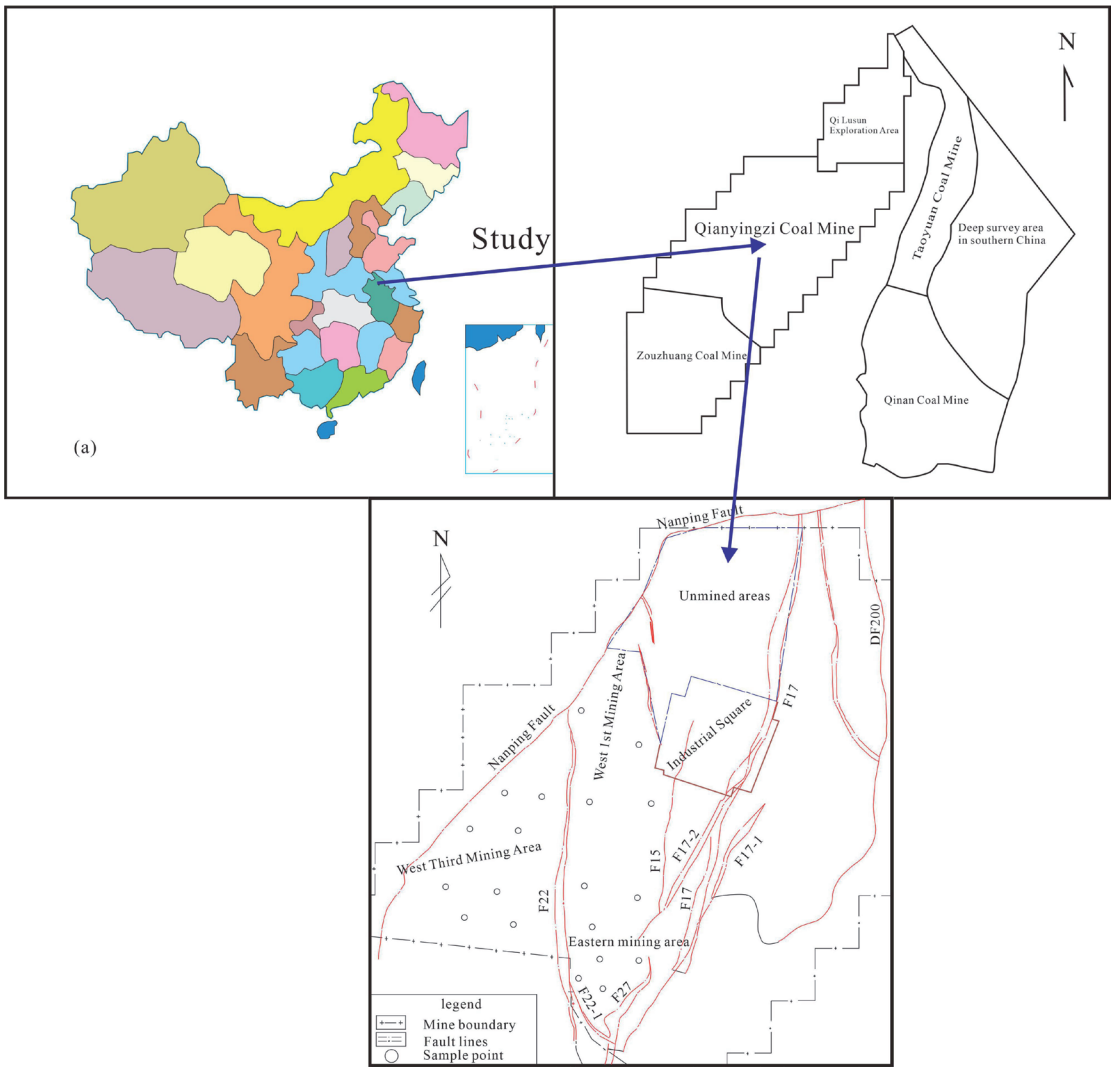

Fig. 1. Geological relationship map of the study area and the sample collection point.

ion chromatograph, with 1.3 mL methanesulfonic acid added to a 1000 mL volumetric flask as the cation eluent. Anions (Cl^-, SO_4^{2-}): Tested using an ICS-900 ion chromatograph with ultrapure water eluent. Hardness and HCO_3^-: Determined through acid-base titration. Quality control measures included verifying instrument stability with standard samples and analyzing duplicate samples to ensure relative deviations remained below 5%.

Water Quality Evaluation Treatment Methods

Selection of Evaluation Indicators

China's Groundwater Quality Standards (GB/T14848-2017) [11] provide the primary framework for assessing groundwater quality. These standards categorize groundwater into five classes based on current quality conditions, human health benchmarks, protection objectives, and stringent requirements for domestic, industrial, and agricultural water use.

The selected indicators – total dissolved solids (TDS), chloride (Cl^-), sodium (Na^+), total hardness, pH, and sulfate (SO_4^{2-}) – were chosen for their measurability, comparability, and sensitivity to local water quality conditions. Notably, sodium content represents the sum of Na^+ and K^+ concentrations.

Single Index Evaluation Method

The single-parameter evaluation method [12] serves as a foundational and intuitive approach for groundwater quality assessment. This method compares individual indicator concentrations against standardized thresholds to determine compliance. Operationally, it is user-friendly, straightforward, and enables rapid evaluation of specific water quality parameters. Following the worst-case principle [13], the poorest-performing indicator dictates the overall groundwater quality classification.

F-Value Comprehensive Evaluation Method

(1) The F-value method [14] assigns scores F_i to individual components based on measured values and GB/T14848–2017 criteria.

(2) Comprehensive quality is calculated using Equations (1)-(3):

$$F = \sqrt{\frac{\bar{F}^2 * F_{max}^2}{2}} \quad (1)$$

$$\bar{F} = \frac{1}{n}\sum_{i=1}^{n} F_i \quad (2)$$

$$F_{max} = \max\{F_1, F_2, \ldots\ldots, F_n\} \quad (3)$$

where F_i is the score of the i-th indicator, $\bar{F}$ is the erage score, F_{max} is the maximum score, and n is the number of indicators.

(3) Groundwater quality categories are classified as: <0.80 (Class I, excellent); 0.80-2.50 (Class II, good); 2.50-4.25 (Class III, fair); 4.25-7.20 (Class IV, poor); 7.20 (Class V, very poor) [15].

Fuzzy Comprehensive Evaluation Method

The fuzzy comprehensive evaluation method [16], rooted in fuzzy mathematics, quantifies influencing factors via weights and membership degrees, making it suitable for multi-indicator, nonlinear, and uncertain water quality assessments. Key steps include defining factor and evaluation sets, establishing membership functions, constructing fuzzy relation matrices, determining weight matrices, and performing fuzzy synthesis [17].

(1) Establish factor sets and evaluation sets. The factor set for Qianyingzi Coal Mine is defined as U = {pH, total dissolved solids, sodium, chloride, sulfate, total hardness}. The evaluation set V = {I, II, III, IV, V} corresponds to the five groundwater quality classes in GB/T14848–2017.

(2) Establish the membership function of individual factors.

The membership function for Class I water (j = 1) is defined as:

$$r_{i1} = \begin{cases} 1 & x_i \le c_{i1} \\ \frac{c_{i2}-x_i}{c_{i2}-c_{i1}} & c_{i1} \le x_i \le c_{i2} \\ 0 & x_i \ge c_{i2} \end{cases} \quad (4)$$

For Class II.~IV water (j = 2, 3, 4), the membership function is:

$$rij = \begin{cases} 0 & x_i \ge c_{i(j+1)} \\ \frac{x_i - c_{i(j-1)}}{c_{ij} - c_{i(j-1)}} & c_{i(j-1)} \le x_{ij} \le c_{ij} \\ \frac{c_{i(j+1)} - x_i}{c_{i(j+1)} - c_{ij}} & c_{ij} \le x_{ij} \le c_{i(j+1)} \end{cases} \quad (5)$$

For Class V water (j = 5), the membership function is:

$$ri5 = \begin{cases} 0 & x_i \le c_{i4} \\ \frac{x_i - c_{i4}}{c_{i5} - c_{i4}} & c_{i4} \le x_i \le c_{i5} \\ 1 & x_i \ge c_{i5} \end{cases} \quad (6)$$

Where x_i is the measured value (mg/L) of the i-th factor; c_{ij} is the j-th class standard value (mg/L) for the i-th factor; and r_{ij} is the membership degree of the i-th factor to the j-th class. An n×m fuzzy relation matrix R is constructed based on membership degrees of all factors.

(3) Establish a fuzzy relationship matrix.

The fuzzy relation matrix R is defined as:

$$R=\begin{pmatrix} r_{11} & r_{12} & \cdots & r_{1m} \\ r_{21} & r_{22} & \cdots & r_{2m} \\ \vdots & \vdots & & \vdots \\ r_{n1} & r_{n2} & \cdots & r_{nm} \end{pmatrix} \quad (7)$$

(4) Establish a weight matrix of evaluation factors.

Weights and weight matrix calculation. The weight formula is:

$$\alpha_i = \frac{x_i/S_i}{\sum_i^n x_i/S_i} \quad (8)$$

Where S_i is the average of the standard values across all classes for the i-th factor, an n×m weight matrix A is established.

(5) Fuzzy comprehensive evaluation.

Fuzzy matrix composition: Matrix B is obtained via B = A·R. Final evaluation follows the maximum membership principle [18].

Data Analysis Methods

Hydrochemical characteristics were analyzed using mathematical statistics, Piper trilinear diagrams, Gibbs diagrams, and ionic ratios. Descriptive statistics were performed in Excel, while diagrams were generated using Origin 2024 and CorelDRAW.

Results and Discussion

Hydrochemical Characteristics

Statistical results of major ion concentrations, total dissolved solids (TDS), and average pH values for sandstone fissure water samples from Qianyingzi Coal Mine are summarized in Table 1.

The pH ranges from 7.95 to 10.27 (average 8.68), indicating weakly alkaline conditions. TDS values ranged from 935.42 mg/L to 4,645.00 mg/L (mean 2,999.88 mg/L), which is characteristic of saline groundwater [19]. Among cations, alkali metal ions dominate, with concentrations following the order $Na^+ > K^+$. Specifically, sodium concentrations range from 0.40 mg/L to 53.59 mg/L, while potassium ranges from 1.42 mg/L to 24.60 mg/L. The study area belongs to the coal measure strata, which are often rich in pyrite (FeS_2). The oxidation of sulfides is that the S that is insoluble in water enters the water in the form of SO_4^{2-} in large quantities, so the SO_4^{2-} in the groundwater in the study area comes from the dissolution of sedimentary rocks containing gypsum or other sulfates. The reaction is shown in Equation (9). The Na^+ comes from the dissolution of rock salt and other sodium salts in sedimentary rocks.

$$2FeS_2 + 7O_2 + 2H_20 \rightarrow 2FeSO_4 + 4H^+ + 2SO_4^{2-} \quad (9)$$

For anions, sulfate (SO_4^{2-}) is the primary constituent, exceeding bicarbonate (HCO_3^-) in most samples. To assess data variability, the coefficient of variation (CV) was calculated, which is defined as the standard deviation divided by the mean. Higher CV values (>1) indicate greater hydrochemical instability, reflecting diverse formation processes. Notably, the TDS CV was <1, suggesting stable hydrochemical conditions [20]. Similarly, the pH CV is <0.1, implying minimal spatial variability [21]. However, exceptions with CV >1 highlight localized instability in certain components, likely influenced by environmental fluctuations [22].

The Piper trilinear diagram (Fig. 2) was employed to classify hydrochemical types and compare compositional trends [23]. Key observations include: Alkali metals ($Na^+ + K^+$) constitute >80% of cations, exceeding alkaline earth metals ($Ca^{2+} + Mg^{2+}$). Dominant hydrochemical type: $SO4{\cdot}HCO_3$-Na+K. Low Ca^{2+} and Mg^{2+} concentrations, except in rare cases. The water samples exhibit diverse hydrochemical properties. The reasons are as follows: These samples share the same recharge sources and climatic conditions; however, due to different infiltration methods of groundwater, varying burial depths of groundwater runoff, and discrepancies in the water environment and hydrochemical processes, different hydrochemical outcomes arise.

In Fig. 2a), all samples cluster in Zone 2 (alkali metals > alkaline earth metals). Fig. 2b) shows that strong acid anions (SO_4^{2-}, Cl^-) dominate most samples, with weak acids (HCO_3^-) prevalent in a few. Fig. 2c) categorizes samples into Zone 7 (non-carbonate hardness >50%, alkali metals + strong acids) and Zone 8

Table 1. Statistical characteristics of water and water chemistry indexes of sandstone fissures in Qianyingzi Coal Mine.

Statistical items	Na^++K^+	Ca^{2+}	Mg^{2+}	Cl^-	SO_4^{2-}	HCO_3^-	TDS	pH
	mg/L							-
Minimum	388.24	0.40	1.42	104.10	1.65	221.02	935.42	7.95
Maximum	1474.74	53.59	24.60	514.04	2749.08	1090.50	4645.00	10.27
Average value	1007.42	15.38	4.82	160.23	1502.71	494.36	2999.88	8.68
Standard deviation	431.69	13.71	5.18	102.02	1185.91	255.69	1483.89	0.49
Coefficient of Variation	0.43	0.89	1.07	0.64	0.80	0.52	0.49	0.06

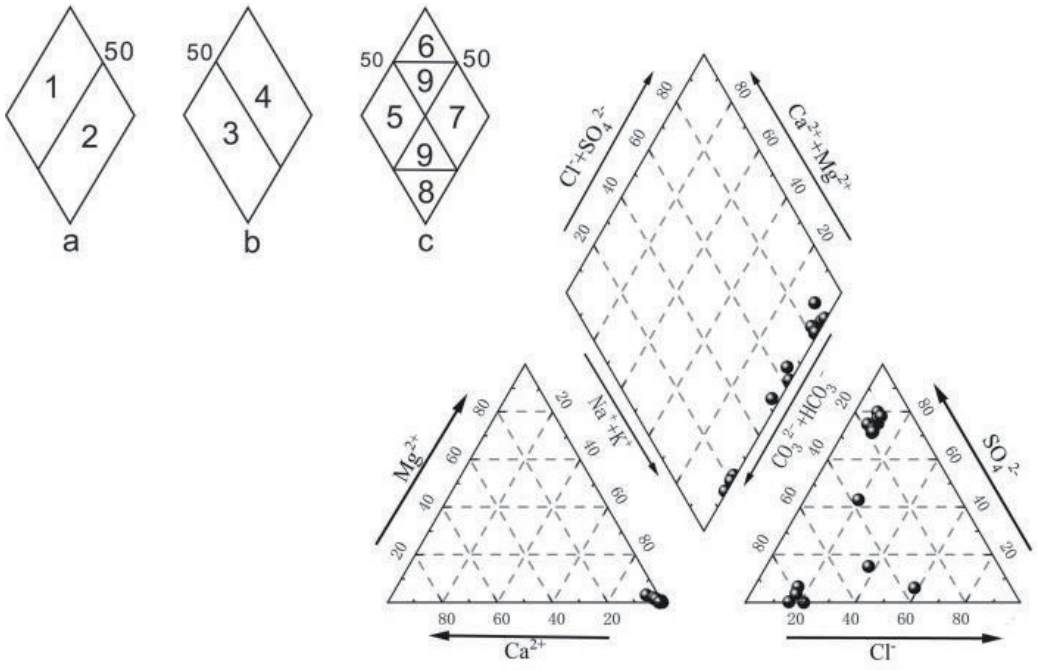

Fig. 2. Piper diagram of a sandstone fissure water sample.

(carbonate hardness >50%, alkaline earth metals + weak acids).

Water-Rock Interaction Mechanisms

Gibbs diagrams (Fig. 3) were used to elucidate hydrochemical controls, classifying mechanisms into three domains: evaporation-crystallization, rock weathering, and atmospheric precipitation [24].

In Fig. 3a), TDS values (1,000-10,000 mg/L) and $Na^+/(Na^+ + Ca^{2+})$ ratios (0.961-0.999) cluster within the evaporation-crystallization zone. Fig. 3b) shows that $Cl^-/(Cl^- + HCO_3^-)$ ratios increase with TDS (<0.5), indicating a transition from rock weathering to evaporation dominance. These patterns collectively suggest that groundwater chemistry is primarily controlled by evaporation-driven water-rock interactions, with minimal influence from weathering or atmospheric precipitation [25].

Ion Ratio Analysis

Analysis of ionic ratios in groundwater provides insights into hydrogeochemical processes [26], as illustrated in Fig. 4.

Na^+/Cl^- ratio of 1 indicates that the halite dissolution dominates groundwater chemistry. Ratios exceeding 1 suggest the presence of additional sodium sources (e.g., other sodium salts) [27].

Fig. 4a) shows that all samples fall below the Na^+/Cl^- = 1 line, implying contributions from silicate dissolution or cation exchange adsorption, where

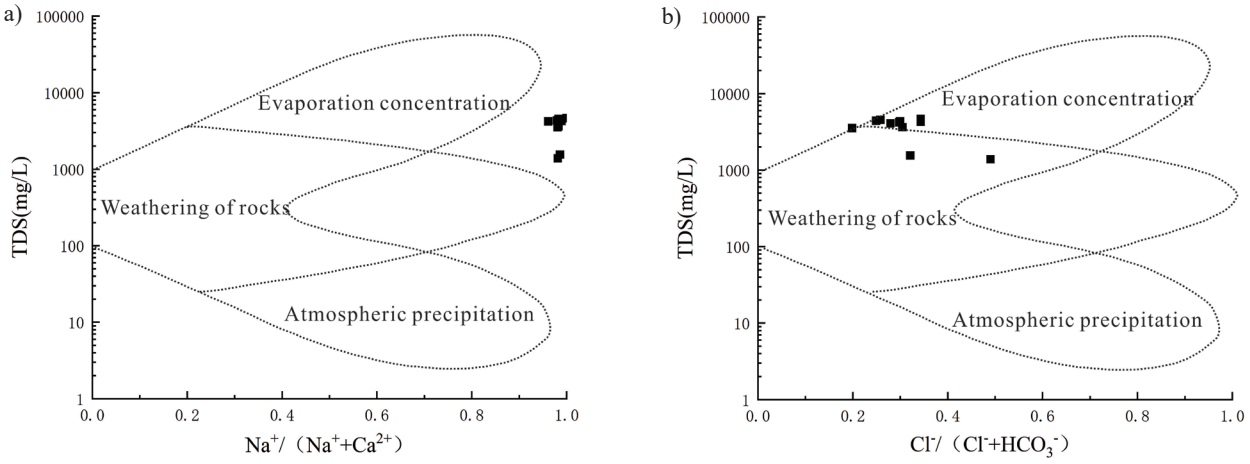

Fig 3. Gibbs plot of the study area.

Na^+ replaces adsorbed Ca^{2+}/Mg^{2+}, elevating Na^+ concentrations [28]. These may include silicate dissolution or cation exchange adsorption occurring in the fissure water. Specifically, cation exchange adsorption replaces Ca^{2+} and Mg^{2+} in the water with Na^+ from rock-soil particles, thereby increasing the concentration of Na^+ in the aqueous phase. It is therefore concluded that, in the study area, the Na^+ in sandstone fissure water originates not only from rock salt dissolution but also from additional processes such as cation exchange adsorption.

$(Ca^{2+} + Mg^{2+})/HCO_3^-$ ratio of 1 suggests carbonate (calcite, dolomite) and sulfate (gypsum, anhydrite) mineral dissolution [29]. Fig. 4b) reveals $(Ca^{2+} + Mg^{2+})/(HCO_3^- + SO_4^{2-})$ ratios <1, indicating low Ca^{2+}/Mg^{2+} levels due to: (1) limited carbonate sources, (2) oxidation-induced SO_4^{2-} enrichment, (3) silicate weathering, or (4)cation exchange (Na^+ displacing adsorbed Ca^{2+}/Mg^{2+}), corroborating Fig. 4a).

Additionally, the dissolution of sulfate minerals serves as a significant source of ions in groundwater. Therefore, the $(Ca^{2+} + Mg^{2+})/SO_4^{2-}$ ratio is commonly employed to investigate the potential sources of Ca^{2+}, Mg^{2+}, and SO_4^{2-} in groundwater [30]. As illustrated in Fig. 4c), most water samples plot above the $(Ca^{2+} + Mg^{2+})/SO_4^{2-} = 1$ baseline, indicating that the primary source of SO_4^{2-} is not limited to sulfate dissolution but also involves additional contributions. $(Ca^{2+} + Mg^{2+})/HCO_3^-$ ratio of 1 signifies carbonate dissolution [31]. However, low Ca^{2+}/Mg^{2+} ratios in the samples (Fig. 4d) highlight the contributions of silicate weathering.

Collectively, ionic ratios confirm that sulfate dissolution and silicate weathering are the primary ion sources in fissure water.

Water Quality Assessment

Evaluation Results

Nineteen groundwater samples were analyzed using single-parameter, F-value, and fuzzy comprehensive evaluation methods. As summarized in Table 2, both the single-parameter and F-value methods categorized 18 samples (94.7%) as Class V (extremely poor quality) and 1 sample (5.3%) as Class IV (poor quality). The primary pollutants – total dissolved solids (TDS), chloride (Cl^-), and sodium (Na^+) – consistently exceeded the Class V thresholds specified by the Chinese Groundwater Quality Standard (GB/T 14848-2017). For instance, Sample 1 exhibited TDS levels of 2000 mg/L (Class V limit: 1000 mg/L), with Cl^-

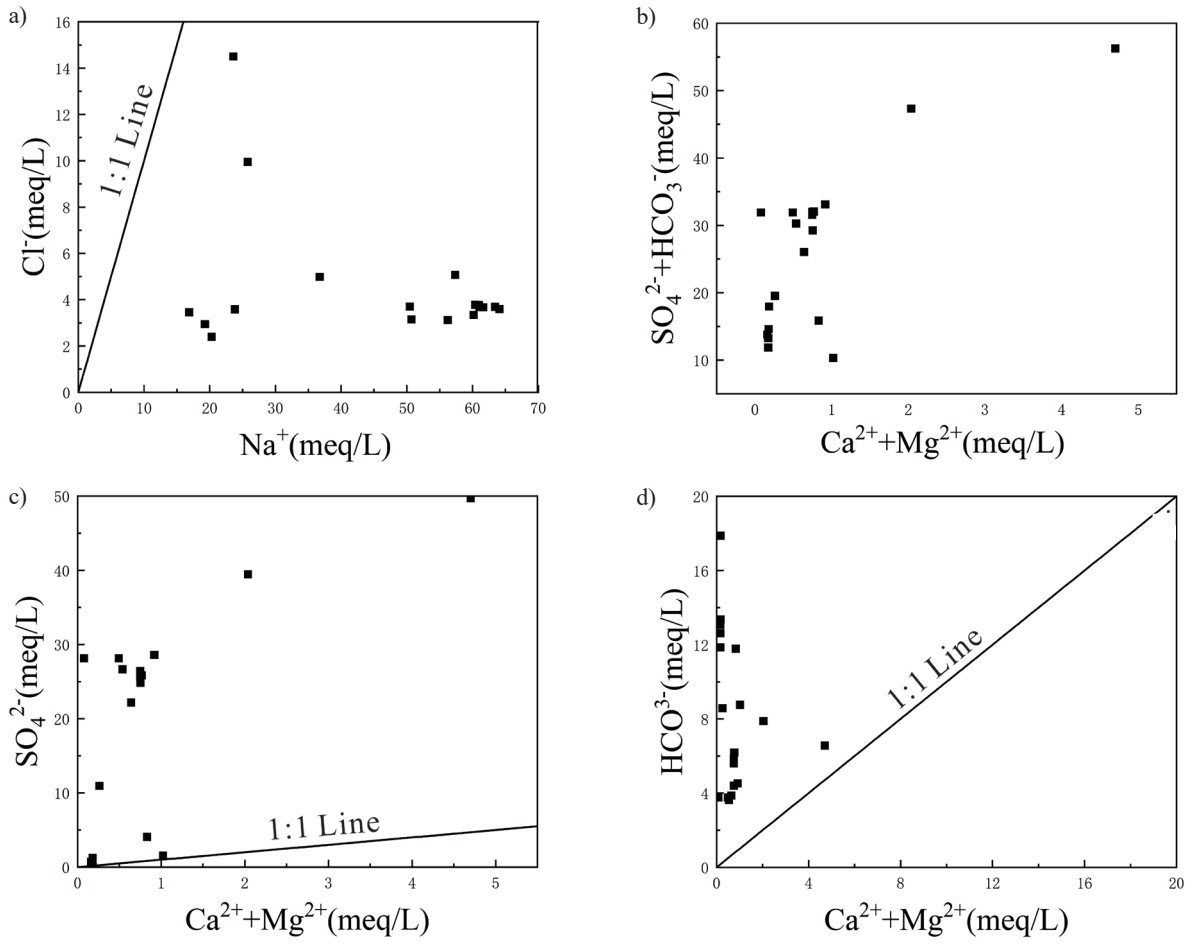

Fig. 4. Ion ratio results in water samples.

Table 2. Water quality evaluation results.

Sample number	Single-index evaluation							Comprehensive quality evaluation			
	TDS	Cl^-	Na^+	Total hardness	pH	Sulfate	Grade	The average value of F	F_{max}	F	Grade
1	V	II	V	I	IV	V	V	6.17	10	8.31	V
2	V	II	V	I	IV	V	V	6.17	10	8.31	V
3	IV	V	V	I	III	I	V	4.83	10	7.85	V
4	IV	V	V	I	IV	III	V	5.84	10	8.19	V
5	V	II	V	I	III	V	V	5.67	10	8.13	V
6	V	II	V	I	III	V	V	5.67	10	8.13	V
7	III	II	III	I	IV	I	IV	2.17	6	4.51	IV
8	IV	II	V	I	IV	II	V	4.00	10	7.62	V
9	IV	II	V	I	IV	II	V	4.00	10	7.62	V
10	IV	II	V	I	IV	II	V	4.00	10	7.62	V
11	IV	II	V	I	III	I	V	3.33	10	7.45	V
12	V	III	V	I	IV	V	V	6.50	10	8.43	V
13	V	II	V	I	V	V	V	6.83	10	8.56	V
14	V	II	V	I	IV	V	V	6.17	10	8.31	V
15	V	II	V	I	V	V	V	6.83	10	8.56	V
16	V	II	V	I	IV	V	V	6.17	10	8.31	V
17	V	II	V	I	III	V	V	5.67	10	8.13	V
18	V	II	V	I	III	V	V	5.67	10	8.13	V
19	V	II	V	I	IV	V	V	6.17	10	8.31	V

and Na^+ concentrations reaching 500 mg/L and 400 mg/L, respectively. Furthermore, pH fluctuations (Class III-V) and elevated sulfate levels indicated potential risks of acidification and sulfate contamination.

The F-value method generated a composite pollution index (F) by aggregating weighted parameters, with all samples exceeding the threshold value of 7.0 (scores >7.45). However, this method's reliance on expert-assigned weights (e.g., 30% for TDS) introduced subjectivity, potentially distorting the evaluation outcomes.

In contrast, the fuzzy evaluation method (Table 3) employed membership functions – mathematical tools that quantify uncertainties in classification – to achieve higher precision. For example, Sample 1 demonstrated a 98.42% membership probability in Class V, confirming severe contamination. Overall, 15 samples (79%) were unambiguously classified as Class V, while 4 samples (21%) were assigned to Class IV due to marginal improvements in parameters such as pH. These results aligned with the single-parameter classification but better captured subtle parameter variations through probabilistic modeling.

Comparative Analysis and Recommendations

Methodological disparities stem from distinct theoretical foundations, such as:

Single-parameter approach: Although conservative, this method neglects parameter synergies [32]. For example, Sample 7 was erroneously classified as Class IV under this method due to the neutralizing effect of pH (Class IV) and sulfate (Class I). In contrast, the fuzzy logic method correctly assigned Class IV by integrating multi-parameter weights.

F-value method: While linear weighting accounts for parameter interactions, it is prone to subjective weight allocation (e.g., 10% for Cl^-), which can potentially lead to underestimating pollutant impacts.

Fuzzy evaluation: This method utilizes membership functions and fuzzy matrices to address data uncertainty and nonlinear relationships. In Sample 3, TDS (Class IV) combined with Cl^- (Class V) yielded a 71.77% membership probability in Class V, consistent with observed contamination levels.

In accordance with WHO and EU guidelines, fuzzy methods demonstrate superior performance in multi-pollutant scenarios. Future research should focus on two priorities: (1) incorporating machine learning algorithms for dynamic weight optimization to reduce subjectivity and (2) enhancing real-time monitoring systems to improve data reliability.

The severe groundwater contamination identified in this study necessitates urgent remediation measures, including industrial emission controls and the implementation of constructed wetlands. These findings

Table 3. Fuzzy comprehensive evaluation results.

Fuzzy comprehensive evaluation results of fracture water quality						
Sample	I	II	III	IV	V	The grade of the water quality
1	0.003028	0.012691	0.000022	0.000033	0.984226	V
2	0.000116	0.013305	0.005721	0.000010	0.980848	V
3	0.010696	0.000052	0.016133	0.255445	0.717673	V
4	0.000037	0.003856	0.027155	0.111049	0.857902	V
5	0.005753	0.008161	0.000043	0.000000	0.986043	V
6	0.004735	0.007194	0.000039	0.000000	0.988033	V
7	0.016136	0.034503	0.078100	0.871261	0.000000	IV
8	0.015363	0.018459	0.023891	0.628704	0.313582	IV
9	0.017558	0.018033	0.025566	0.733522	0.205321	IV
10	0.017795	0.017873	0.025584	0.736016	0.202732	IV
11	0.062161	0.144221	0.110797	0.213378	0.469442	V
12	0.000361	0.020996	0.007704	0.019370	0.951569	V
13	0.004200	0.008175	0.000022	0.000022	0.987580	V
14	0.003449	0.009308	0.000000	0.000027	0.987216	V
15	0.002470	0.010473	0.000027	0.000018	0.987013	V
16	0.002406	0.010125	0.000000	0.000000	0.987469	V
17	0.003141	0.010219	0.000043	0.000000	0.986597	V
18	0.002805	0.011060	0.000043	0.000000	0.986092	V
19	0.002756	0.011286	0.000043	0.000002	0.985913	V

also underscore the need for transregional water resource management, particularly in mining or industrial zones with analogous hydrogeological conditions.

Conclusions

This study systematically analyzed 19 sandstone fissure water samples from the Qianyingzi Coal Mine using statistical methods, hydrochemical classification, and diagrammatic analyses. The main findings are summarized as follows:

(1) Hydrochemical Characteristics: The fissure water exhibits weakly alkaline and saline properties, with hydrochemical composition dominated by Na^+ and SO_4^{2-}. These characteristics suggest significant influence from external inputs, likely linked to mining activities.

(2) Hydrochemical Classification: Piper trilinear diagrams classify the water as $SO_4 \cdot HCO_3$-Na+K type. Notably, Ca^{2+}/Mg^{2+} concentrations are generally low, except in localized areas where mineral dissolution processes may dominate.

(3) Formation Mechanisms: Gibbs diagrams combined with ionic ratio analyses indicate that evaporation-driven processes primarily control water chemistry. Key ion sources include halite dissolution, silicate weathering, and cation exchange, reflecting both natural and anthropogenic influences.

(4) Water Quality Status: Based on the Chinese Groundwater Quality Standard (GB/T 14848-2017), 79% of samples were classified as Class V (heavily polluted), rendering them unsuitable for drinking or irrigation. Mining operations – particularly wastewater discharge and mineral leaching – were identified as major contributors to contamination.

Acknowledgments

This study was supported by the following projects: Open Fund of Coal Industry Engineering Research Center for Exploration and Early Warning of Mine Water Disaster (Grant No.2024-CIERC-07), and the Anhui Excellent Young Teacher Training Project (YQYB2024075), the Academic and Technical Leader Reserve Candidate Program (2024XJHB08), the Drilling Engineering Technology Research Center of Suzhou University (2024PT04), the Quality engineering project of Anhui Province(2023jcjs140), and the Key Projects of Natural Science Research in Anhui Universities (2023AH052224, 2024AH051819), the Anhui Provincial Program for Science and Engineering

Faculty to Undertake Practical Training in Enterprises (2024jsqygz117), and the Suzhou University Quality Engineering Project (szxy2023xxhz01, szxy2022ctzy01), the National College Students Innovation and Entrepreneurship Training Program (202410379064S), and Provincial College Students Innovation and Entrepreneurship Training Program (S202410379176S).

Conflict of Interest

The authors declare no conflict of interest.

References

1. ZAHIDAH A., PUTRA E.P.D., WILOPO W. Hydrochemical characteristics of groundwater and the implications for conceptual models of aquifers: a study of Cangkringan, Yogyakarta, Indonesia. Hydrological Sciences Journal, **70** (5), 761, **2025**.
2. SAURABH S., RAMSHA K., KUMAR S.V. Appraisal of groundwater chemistry, its suitability for crop productivity in Sonipat district and human health risk evaluation. Human and Ecological Risk Assessment: An International Journal, **29** (2), 507, **2023**.
3. LIANG Y., WU B., WANG J. Optimization of recharge parameters for foundation pit engineering based on orthogonal test and fuzzy analytical hierarchy process-value engineering method. Tunnel Construction, **41** (9), 1492, **2021**.
4. ETIKALA B., VANGALA S., MADHAV S. Groundwater geochemistry using modified integrated water quality index (IWQI) and health indices with special emphasis on nitrates and heavy metals in southern parts of Tirupati, South India. Environmental Geochemistry and Health, **46** (11), 465, **2024**.
5. QU J., LIN J., WANG J. Analysis of the evolution and causes of groundwater chemistry after ecological water replenishment of the Jialu River, China. Scientific Reports, **14** (1), 18759, **2024**.
6. KUMAR T.C., SHAHNUL M.I., CHANDRA G.G. Human health risk and hydro-geochemical appraisal of groundwater in the southwest part of Bangladesh using GIS, water quality indices, and multivariate statistical approaches. Toxin Reviews, **42** (1), 285, **2023**.
7. DHEERAJ P.V., SINGH S.C., ALAM A. Hydrogeochemical quality investigation of groundwater resource using multivariate statistical methods, water quality indices (WQIs), and health risk assessment in Korba Coalfield Region, India. Stochastic Environmental Research and Risk Assessment, **39** (3), 1, **2025**.
8. ADIMALLA N., VASA K.S., LI P. Evaluation of groundwater quality, Peddavagu in Central Telangana (PCT), South India: an insight of controlling factors of fluoride enrichment. Modeling Earth Systems and Environment, **4** (2), 841, **2018**.
9. SHUJIAN L., HE S., ZHI L. Hydrochemical characteristics and groundwater quality in the thick loess deposits of China. Environmental Science and Pollution Research International, **29** (6), 8831, **2021**.
10. YU Y., YAN B., TUO Y. Chemical evolution characteristics and influencing factors of groundwater in the saline and fresh water funnel area in Hengshui City, North China. Scientific Reports, **15** (1), 3276, **2025**.
11. YOUNAS F., SARDAR F.M., ULLAH Z. Assessment of groundwater chemistry to predict arsenic contamination from a canal commanded area: applications of different machine learning models. Environmental Geochemistry and Health, **47** (2), 46, **2025**.
12. LUPI F., HERRIGES J.A,, KIM H., STEVENSON R.J. Getting off the ladder: Disentangling water quality indices to enhance the valuation of divergent ecosystem services, Proceedings of the National Academy of Sciences of the United States of America, **120** (18), e2120261120, **2023**.
13. HONGYUN Z., SUN H., BIAN K. Seasonal Variation Characteristics of Karst Groundwater Chemistry and Water Quality Assessment in the Northern Part of the Baiquan Spring Area. Journal of Water Chemistry and Technology, **46** (1), 80, **2024**.
14. HEENA S., CHAND S.R., SUDHIR K. Spatial variation in groundwater quality and health risk assessment for fluoride and nitrate in Chhotanagpur Plateau, India. Environmental Monitoring and Assessment, **195** (8), 921, **2023**.
15. GOLLA, SWAMY V., BADAPALLI. Evaluation of water quality for drinking and irrigation purposes and Fluoride Health Hazard Risk Assessment (HHRA) in parts of semi-arid regions in the south-eastern part of India. International Journal of Energy and Water Resources, **6** (4), 1, **2021**.
16. ZHAO X.Y.Z. Fuzzy Comprehensive Evaluation of Groundwater Quality Based on GIS of Yinkeng area. South China Geology, **38** (2), 330, **2022**.
17. ZHANG X.Y., CAI Z.Z., TAN B.X. Hydrochemical Characteristics of Shallow Groundwater and Identification of Water Quality Types in the Dawen River Basin. Huan Jing Ke Xue= Huanjing Kexue, **46** (2), 821, **2025**.
18. HE S., WU J. Hydrogeochemical Characteristics, Groundwater Quality, and Health Risks from Hexavalent Chromium and Nitrate in Groundwater of Huanhe Formation in Wuqi County, Northwest China. Exposure and Health, **11** (2), 125, **2019**.
19. ZAHID M., MUNEER A., NADEEM A.B., RAKESH M., ANAYAT A.Q. Hydro-chemical Characteristics of Melt Water Draining from Glaciers of Rongdo Basin, Shyok Valley, Ladakh. Journal of the Geological Society of India, **99** (4),459, **2023**.
20. AHMED A., ALSHAMIS D., ARMAN H. Identifying the factors controlling surface water and groundwater chemical characteristics and suitability in the East Nile Delta Region, Egypt. Applied Water Science, **15** (4),73, **2025**.
21. GUO X.G., DAI D.Y., XU L. Chemical Characteristics and Genetic Analysis of Karst Groundwater in the Beijing Xishan Area. Huan Jing Ke Xue= Huanjing Kexue, **45** (2), 802, **2024**.
22. XIAOQING C., HAITAO Z., YOUJING C. Hydrochemical characteristics and processes of groundwater in the Cenozoic pore aquifer under coal mining. Environmental Science and Pollution Research International, **30** (12), 33334, **2022**.
23. JIUTAN L., ZONGJUN G., ZHENYAN W. Hydrogeochemical processes and suitability assessment of groundwater in the Jiaodong Peninsula, China. Environmental Monitoring and Assessment, **192** (6), 384, **2020**.
24. ZHANG Z., LIU F., CHEN S. Hydrogeochemical and isotopic insights into groundwater evolution in the agricultural area of the Luanhe Plain. Environmental Earth Sciences, **83** (20), 593, **2024**.

25. SINGH M., WADHWA V., BATRA L. A chemometric and ingestion hazard prediction study of groundwater in proximity to the Bandhwari landfill site, Gurugram, India. Journal of Water and Health, **22** (1), 52, **2024**.
26. PANDURANG B., JYOTHI V., PARAS R.P., SONI A., PADMAKAR C., QUAMAR R., RAMESH J., GOHEL V., MISHRA A. Integrated hydrochemical and ERT approach for seawater intrusion study in a coastal aquifer: a case study from Jafrabad Town, Gujarat State, India. Environmental Monitoring and Assessment, **193** (9), 558, **2021**.
27. LI H., ZHANG W., WANG Y. Chemical characteristics and evolution of groundwater in northeastern margin of the Tibetan Plateau, China. Environmental Geochemistry and Health, **47** (1), 11, **2024**.
28. FARAH K., NOUHA K., ABDELMALEK D. Hydrogeochemical assessment and modeling of groundwater processes and pollution: a case study of the Grombalia aquifer in Northeast Tunisia. Modeling Earth Systems and Environment, **10** (3), 3573, **2024**.
29. MARTA T., MAREK B., SEBASTIAN B. Influence of natural and anthropogenic factors on the chemical composition of shallow groundwater in the city of Wrocław, south-west Poland. Geologos, **28** (3), 191, **2022**.
30. MONJIL R., UTTAM G., DEVOJIT B. Groundwater Chemistry of the River Terrace Springs along Himalayan Foothills in and around Pasighat, Arunachal Pradesh, India. Journal of the Geological Society of India, **99** (6), 875, **2023**.
31. FENTA N., ALEMU Y., SEWALE A.B. Hydrogeochemical processes and groundwater evolution in complex volcanic highlands and alluvio-lacustrine deposits (Upper Blue Nile), Ethiopia. Environmental Science and Pollution Research International, **30** (23), 63953, **2023**.
32. ZHOU D., YANG H., SAVICHEV O.G., JIN K., WU Y. Comparative Analysis of the Chemical Composition of Surface and Groundwater in the Poyang Lake Catchment Area (China). Geography and Natural Resources, **45** (1), 101, **2024**.